**Advances in Nano Research**, *Vol. 15, No. 6 (2023) 567-577*
https://doi.org/10.12989/anr.2023.15.6.567


# Analysis of the mechano-bactericidal effects of nanopatterned surfaces on implant-derived bacteria using the FEM

Ecren Uzun Yaylacı*[1], Mehmet Emin Özdemir[2], Yılmaz Güvercin[3], Şevval Öztürk[4] and Murat Yaylacı[4,5]

[1]*Faculty of Engineering and Architecture, Recep Tayyip Erdogan University, 53100, Rize, Turkey*
[2]*Department of Civil Engineering, Cankiri Karatekin University, 18100, Çankırı, Turkey*
[3]*Trabzon Kanuni Training and Research Hospital, Department of Orthopaed & Traumatol, 61000, Trabzon, Turkey*
[4]*Department of Civil Engineering, Recep Tayyip Erdogan University, 53100, Rize, Turkey*
[5]*Biomedical Engineering MSc Program, Recep Tayyip Erdogan University, 53100, Rize, Turkey*

(*Received July 9, 2023, Revised September 19, 2023, Accepted September 20, 2023*)

**Abstract.** The killing of bacteria by mechanical forces on nanopatterned surfaces has been defined as a mechano-bactericidal effect. Inspired by nature, this method is a new-generation technology that does not cause toxic effects and antibiotic resistance. This study aimed to simulate the mechano-bactericidal effect of nanopatterned surfaces' geometric parameters and material properties against three implant-derived bacterial species. Here, *in silico* models were developed to explain the interactions between the bacterial cell and the nanopatterned surface. Numerical solutions were performed based on the finite element method. Elastic and creep deformation models of bacterial cells were created. Maximum deformation, maximum stress, maximum strain, as well as mortality of the cells were calculated. The results showed that increasing the peak sharpness and decreasing the width of the nanopatterns increased the maximum deformation, stress, and strain in the walls of the three bacterial cells. The increase in spacing between nanopatterns increased the maximum deformation, stress, and strain in *E. coli* and *P. aeruginosa* cell walls it decreased in *S. aureus*. The decrease in width with the increase in sharpness and spacing increased the mortality of *E. coli* and *P. aeruginosa* cells, the same values did not cause mortality in *S. aureus* cells. In addition, it was determined that using different materials for nanopatterns did not cause a significant change in stress, strain, and deformation. This study will accelerate and promote the production of more efficient mechano-bactericidal implant surfaces by modeling the geometric structures and material properties of nanopatterned surfaces together.
**Keywords:** finite element method; implant-derived bacteria; mechano-bactericidal; nanopatterned surface

## 1. Introduction

In recent years, the increasing use of permanent implants has positively affected patient's life. However, in orthopedics, implant-associated infections are considered one of the main factors limiting the use of implants (de Breij *et al*. 2016). Implants are ideal surfaces for bacteria to form biofilms. Infections begin when pathogenic micro-organisms are attached to the implant surface and colonize there. Gram-positive *Staphylococcus aureus* can form a biofilm in orthopedic implants, heart valves, and devices such as pacemakers and can be isolated from prosthetic materials. The spread of bacteria on the implant is direct or hematogenous. Obesity, immune system deficiency, malignancy, and repeated surgeries of the same region increase the risk of *S. aureus* infections (Kuiper *et al*. 2014). *Escherichia coli* is a Gram-negative bacteria that normally lives in the intestinal flora and can cause extra-abdominal infections with various factors. *E. coli*, like many bacteria forms a biofilm, attaches to the implant surface, and colonizes, causing infections (Crémet *et al*. 2012). *Pseudomonas aegrinosa* is another Gram-negative bacteria that causes implant-associated infections.

*Corresponding author, Assosiate Professor,
E-mail: ecren.uzunyaylaci@erdogan.edu.tr

*P. aeruginosa* is considered one of the most difficult bacteria to treat in medicine, with its ability to develop multi-drug resistance, biofilm formation ability, and virulence mechanisms such as forming colony variants (Cerioli *et al*. 2020).

Prolonged use of antibiotics in surgical implant procedures causes systemic toxicity (Hansen *et al*. 2012). Persistent infections may cause more operations as well as complicate existing treatment. Implant-related infections are difficult to treat, so the most effective solution is to develop methods to prevent infection (Chouirfa *et al*. 2019). In the past, "release-based coatings" have been used to inhibit bacterial colonization (Li *et al*. 2018). However, in this method, problems such as cytotoxicity, inflammatory responses, and bacterial resistance developed due to the uncontrolled release of the drug in the coating (Westberg *et al*. 2015). Therefore, there has been increased interest in mechano-bactericidal approaches, an innovative and alternative method inspired by the prevention of bacterial colonization and biofilm formation by naturally structured nano-surfaces (Cui *et al*. 2021, Alameda *et al*. 2022).

Mechano-bactericidal activity is affected by the cell wall structure and size of the bacteria as well as the properties of the nanostructures on the material surface. (Zhou *et al*. 2021, Linklater *et al*. 2021). In the mechano-bactericidal effect, the interactions between the nano-surfaces and the cell lead to physical rupture of the cell wall, leakage of the



ISSN: 2287-237X (Print), 2287-2388 (Online)

cytoplasm, and eventually death of the bacteria (Pogodin *et al*. 2013, Roy and Chatterjee 2021). The interaction of bacteria and nano-surfaces is a dynamic process and is under the influence of multiple factors. There is a consensus that the bactericidal effect of nano-patterned surfaces is the result of/results from mechanical forces (Ivanova *et al*. 2020). However, it is very complicated to simultaneously characterize the effect of many factors on the bactericidal mechanism (Alameda *et al*. 2022). Therefore, computer-aided numerical simulations, in which many factors can be processed simultaneously, are widely used to eliminate uncertainties.

The finite element method (FEM) is a mathematical method used in engineering approaches in many fields, especially medicine, and dentistry, and in solving complex engineering problems (Pandey *et al*. 2019, Eltaher *et al*. 2019, Mehar and Panda 2019, Pandey *et al*. 2019, Altabey *et al*. 2020, Yaylacı *et al*. 2021, Bouafia *et al*. *2021*, Kuma *et al*. 2021, Yaylacı 2022, Yaylacı *et al*. 2022a, b, c, Güvercin *et al*. 2022a, b, Xia *et al*. 2023, Zagane *et al*. 2023, Uzun Yaylacı *et al*. 2023). In some studies, finite element analysis was used to calculate interactions between bacteria and nanopatterned surfaces (Mirzaali *et al*. 2018, Velic *et al*. 2021, Cui *et al*. 2021). Although the bactericidal effect of the geometric structure of nanopatterned surfaces is known, there are few studies examining the effects of both geometric features and material properties together.

This study aimed to simulate the bactericidal effect of the geometric parameters (peak sharpness, height, width, and spacing) and material properties (chrome-cobalt, zirconium, titanium, and magnesium) of nanopatterned surfaces against three implant-derived bacterial species (*E. coli*, *P. aeruginosa*, and *S. aureus*). Cell-surface interactions were calculated by numerical analysis based on FEM methods. For this purpose, elastic and creep deformation models of *E. coli*, *P. aeruginosa*, and *S. aureus* cells adhered to the nanosurface were created, and cell deformation, stress, strain, and mortality were calculated.

In this study, the model was designed using the ANSYS Workbench package program (ANSYS 2013). The kinetic reaction of the material under various mechanical stresses and strains was analyzed using the finite element module. The FEM analysis applied in this study aimed to simulate the interactions between bacteria and the nanopatterned surfaces.

*E. coli*, *P. aeruginosa*, and *S. aureus* were used as model bacteria to investigate cell-surface interactions. Gram-negative and rod-shaped *E. coli* cell is approximately 2 µm length and 0.5 µm in diameter (Vadillo-Rodriguez *et al*. 2009) with a cell wall thickness of 6 nm (Turner *et al*. 2013). *P. aeruginosa* is a Gram-negative and rod-shaped bacteria. The *P. aeruginosa* cell is 0.5 µm in diameter, 1.5 µm in length (Zhao *et al*. 2022), and 3 nm in cell wall thickness (Turner *et al*. 2013). Gram-positive and cocci-shaped *S. aureus* cell is 0.6 µm in diameter and has a cell wall thickness of 10 nm (Pogodin *et al*. 2013). Fig. 1 shows the schematic illustrations of *E. coli* (A), *P. aeruginosa* (B), and *S. aureus* (C), cells.

Height, width, and spacing were considered the basic geometric parameters for the nanopatterns shown in Fig. 2.

Table 1 Material parameters of model bacteria

| Models | Element Type | Values | Literature |
|---|---|---|---|
| Cytoplasm | Hyperelastic | $D_1$=1666.7 MPa$^{-1}$, $\mu_0 = 2C_{10}$, $C_{10}$=6.21*10$^5$MPa | Mirzaali *et al*. (2018) |
| Bacteria wall | Linear elastic | E=25 MPa, $\nu$=0.16 | Turner *et al*. (2013) Yao *et al*. (1999) |

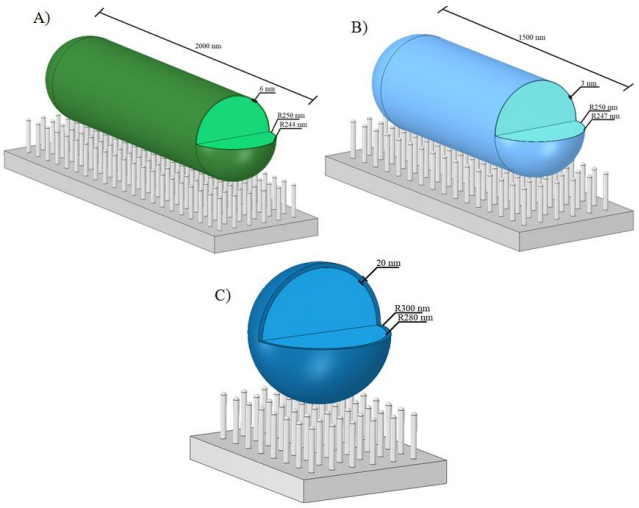


Fig. 1 3D representation of bacteria *E. coli* (A), *P. aeruginosa* (B), and *S. aureus* (C)

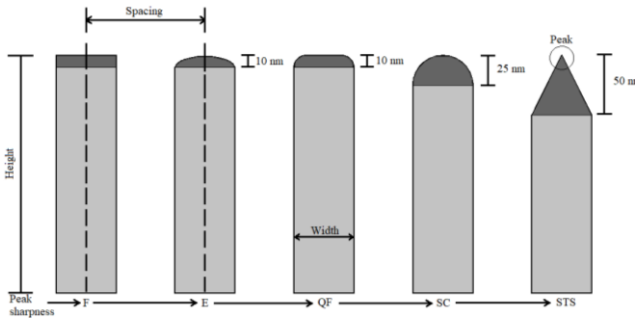


Fig. 2 The schematic illustration of the nano-patterns with different geometries

In many models, the height of the nanopattern does not significantly affect bactericidal activity (Velic *et al*. 2021). In addition, it has been reported that the membrane tension does not change when the height rises above 200 nm (Li 2016). In the analysis, the height of the nanopatterns was fixed at 200 nm. Other parameters, width, peak, and spacing, were chosen to be compatible with the solutions. Peak sharpness was coded as flat: F, ellipse: E, quasi-flat: QF, semicircular: SC, and sharp tip shapes: STS.

The elastic properties of model bacteria used for mechano-bactericidal analysis are given in Table 1.

The properties of the chromium-cobalt, zirconium, titanium, and magnesium materials analyzed in the study are listed in Table 2.

Planes 183 and 182 were assigned from the finite element program library for cell walls and nanopatterns to construct the mesh structure of bacterial models. The number of elements used to obtain the optimum

Table 2 Material parameters of nano-patterns

| Material | Elasticity Module (MPa) | Poisson Ratio | Literature |
|---|---|---|---|
| Chrome-Cobalt (CoCr) | 218000 | 0.33 | Callister and Rethwisch (2013) |
| Zirconium (Zr) | 205000 | 0.22 | Callister and Rethwisch (2013 |

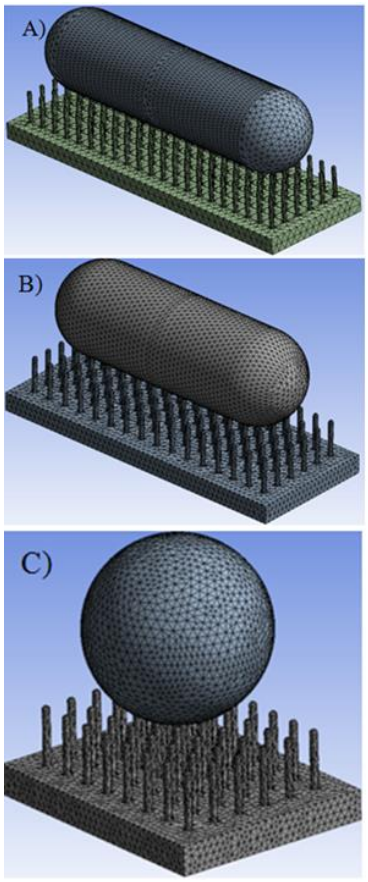


Fig. 3 The finite element mesh structure of *E. coli* (A), *P.aeruginosa* (B), and *S. aureus* (C) cells

convergence value of each mesh structure was 56194 for *E. coli*, 47268 for *P. aeruginosa*, and 27280 for *S. aureus*. In addition, the network structures for *E. coli*, *P. aeruginosa*, and *S. aureus* bacteria contained 94446, 81403, and 50440 nodes, respectively (Fig. 3).

It was assumed that the bacteria were immersed in 5 mm of liquid and placed at the bottom of the medium. Thus, two forces occur: the first is the bacteria's weight, and the second is the hydrostatic pressure from the environment. The equal effect of these forces was applied to the cell wall and cytoplasm as a body force. Buoyancy was ignored as they were minor compared to body forces. Friction between bacteria and nanopatterned surfaces was neglected. A surface-to-surface contact element defined the interaction between bacteria and nanopatterned surfaces. *E. coli*, *P. aeruginosa*, and *S. aureus* were considered to have masses of 1 pg (Cayley *et al*. 1991), 0.4 pg (Ghanbari *et al*. 2016), and 1 pg (Donlan 2002), respectively.

The quality of the resulting mesh structure was checked, and the adequacy and suitability of the element dimensions

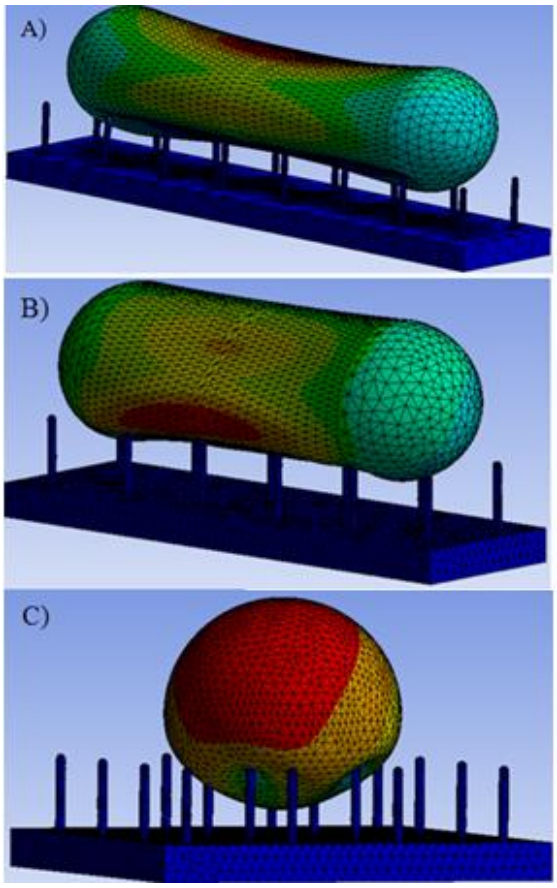


Fig. 4 Finite element models analysis of *E. coli* (A), *P.aeruginosa* (B), and *S. aureus* (C) cells

Table 3 Comparison of the equivalent von Mises strain (maximum)

| Bacteria | Maleki *et al*. (2021) | Present study | $E_{mae}$ |
|---|---|---|---|
| *E. coli* | 0.793 | 0.783 | 1.26 |
| *P. aeruginosa* | 0.452 | 0.445 | 1.55 |

were verified. FEM models of *E. coli*, *P. aeruginosa*, and *S. aureus* cells after analysis are given in Fig. 4.

The turgor pressure values of the model cytoplasms are the representative values used as pressure values while forming the cell wall. This pressure value is according to the literature; it was applied to bacterial models at 0.304 MPa for *E. coli*, 0.15 MPa for *P. aeruginosa*, and 2.533 MPa for *S. aureus (*Whatmore and Reed 1990, Yao *et al*. 2002).

## 3. Results and discussion

FEM analyses were aimed to simulate the interaction of bacterial cells with the nanopatterned surface and to elucidate the effect of geometric and material properties of these nanopatterned surfaces on the mechano-bactericidal effect.

*Validation Study:* To test that the finite element model created in the package program works correctly, it is compared with the numerical results in the literature. A

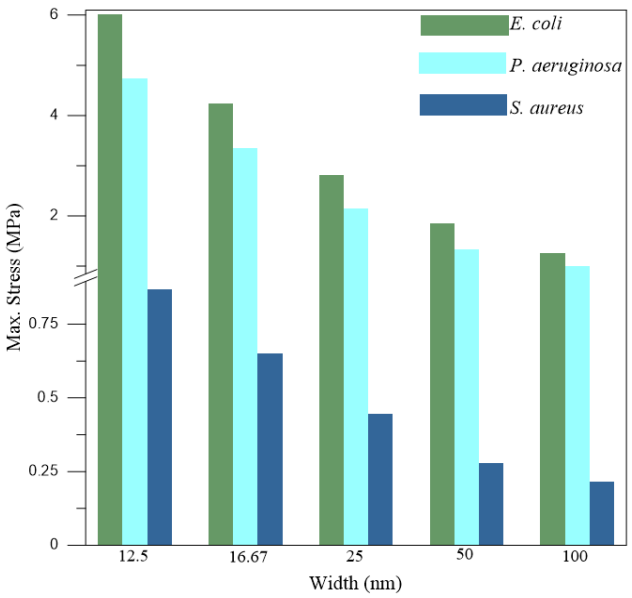


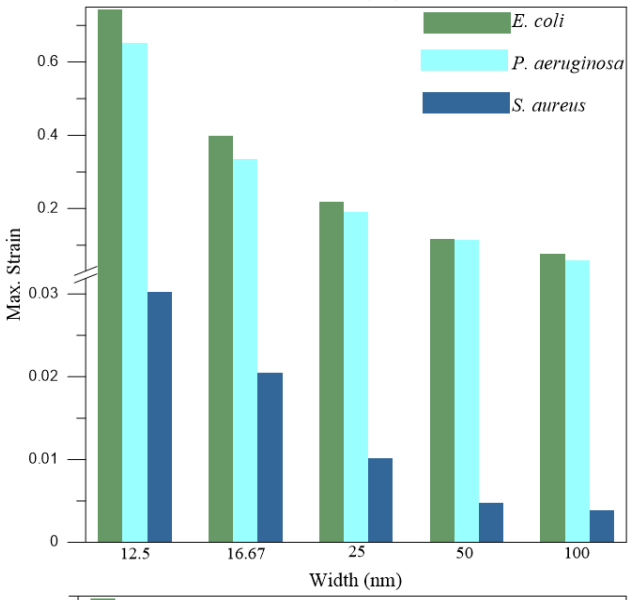


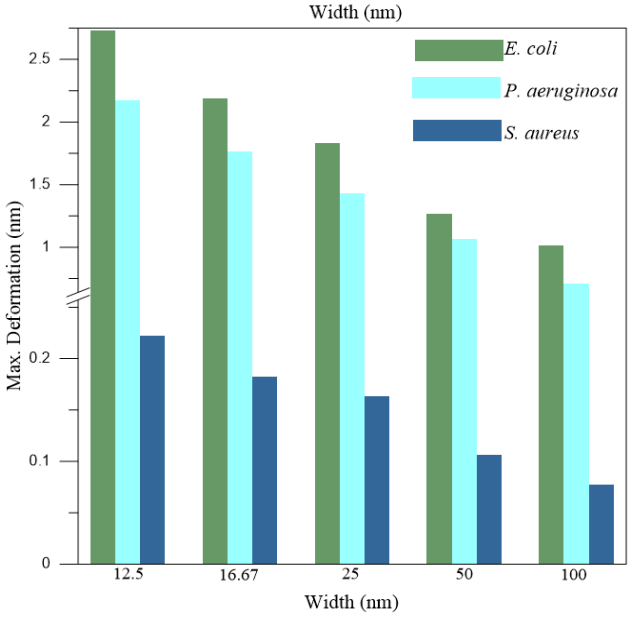


Fig. 5 The variation of the max. stress, max. strain and max. deformation with width

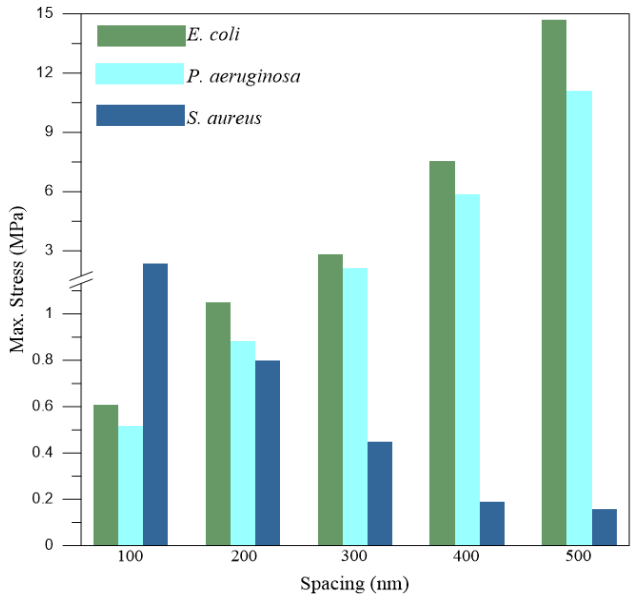


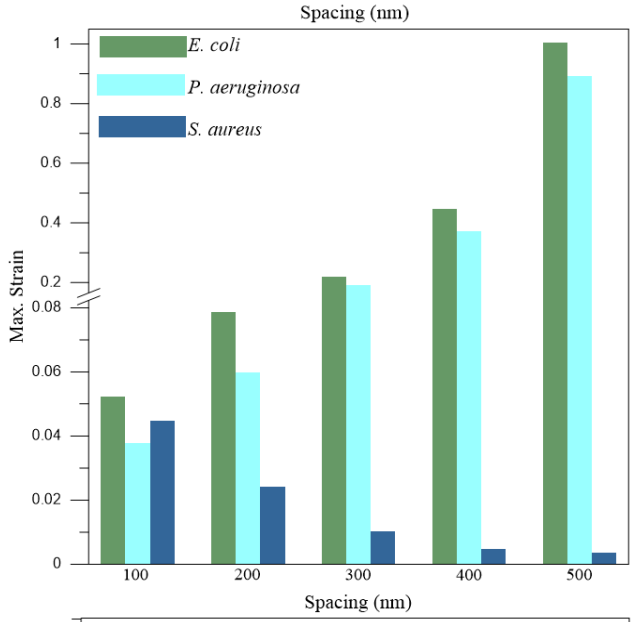


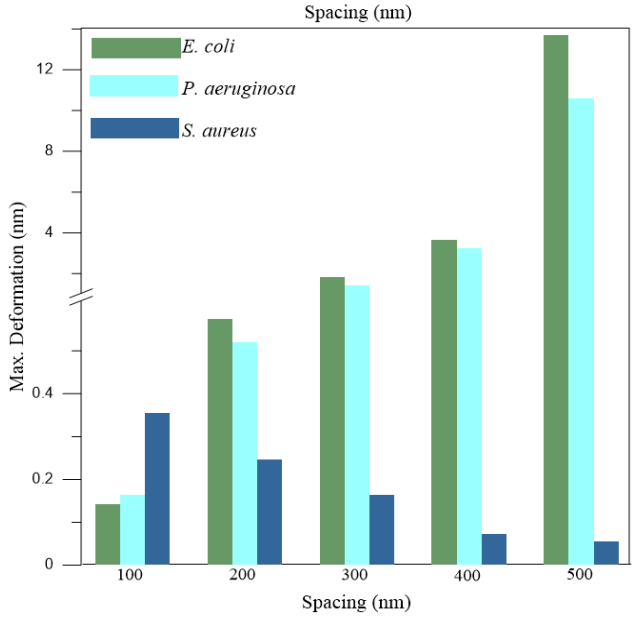


Fig. 6 The variation of the max. stress, max. strain and max. deformation with spacing

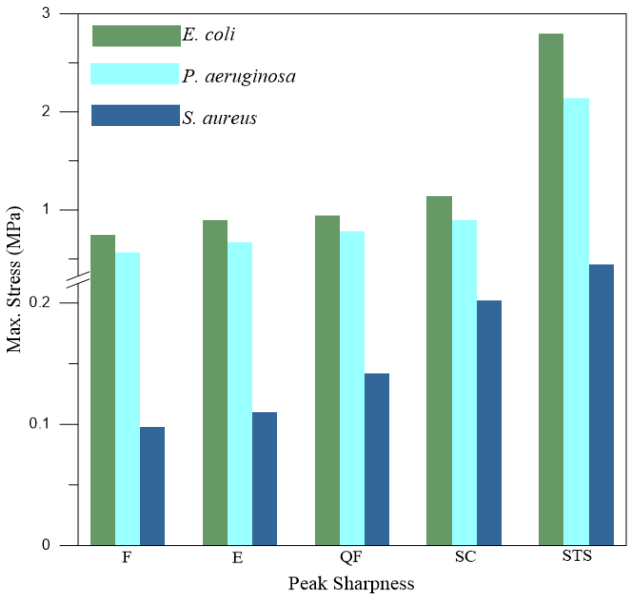


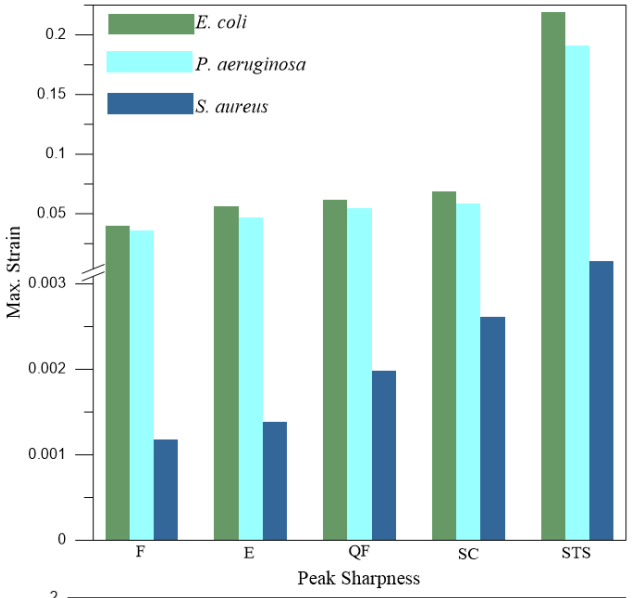


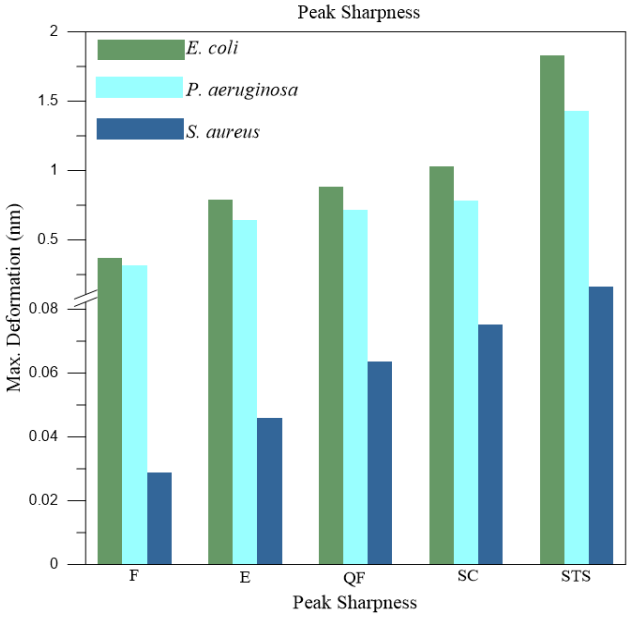


Fig. 7 The variation of the max. stress, max. strain and max. deformation with peak sharpness

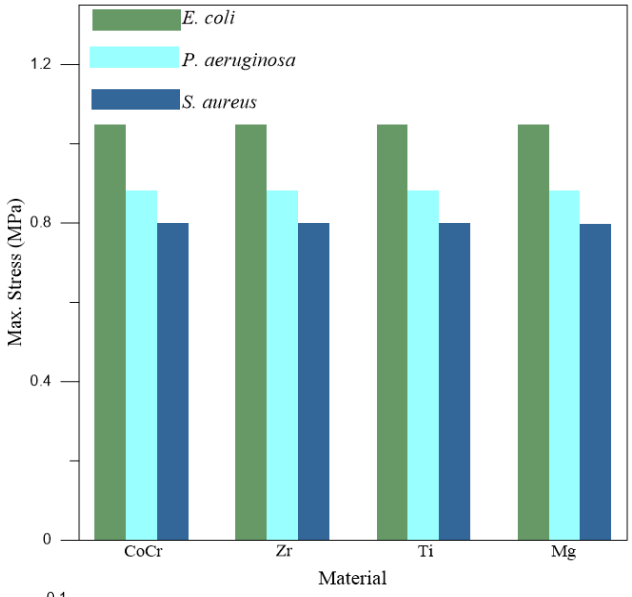


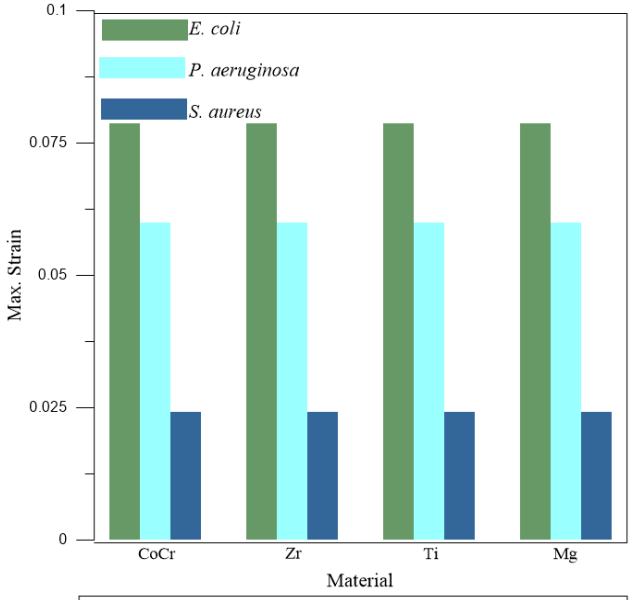


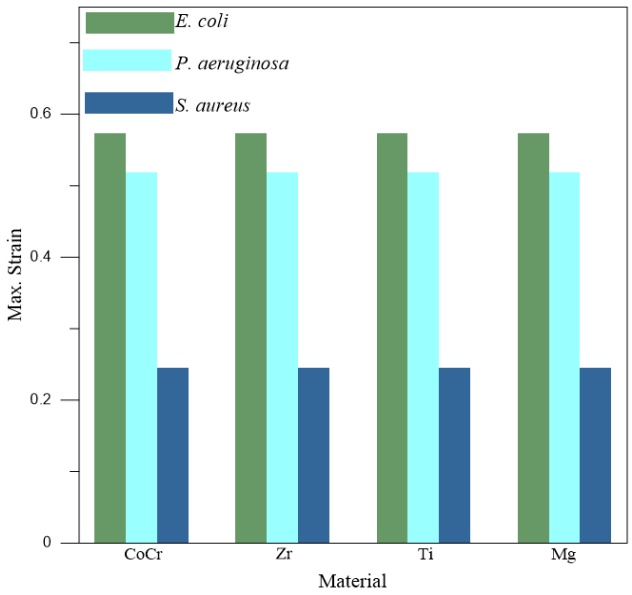


Fig. 8 The variation of the max. stress, max. strain and max. deformation with material

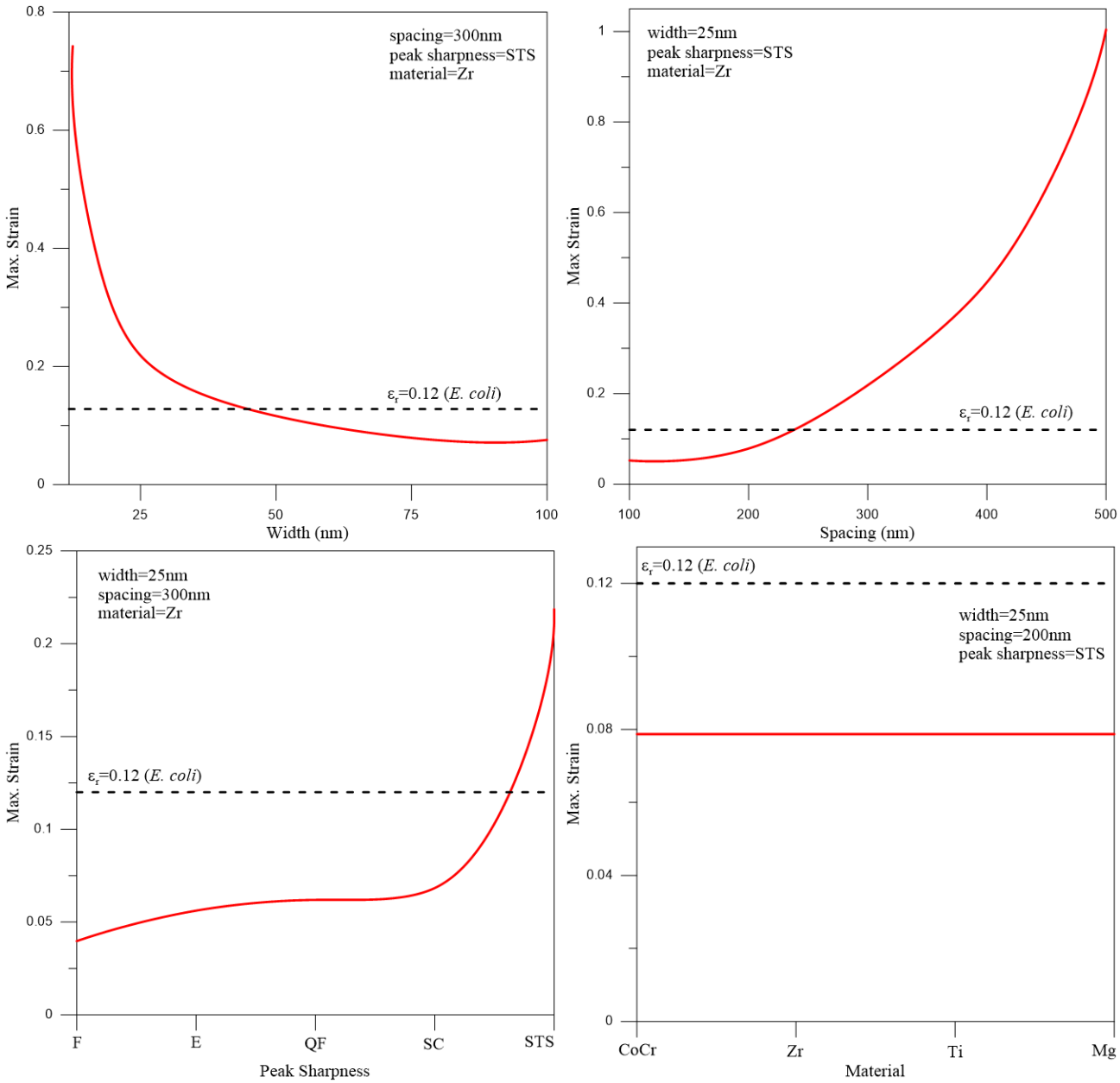


Fig. 9 Parametric analysis (width, spacing, peak sharpness, and material) of E. coli for mortality, taking into account strain

comparison of the closeness of the results was made based on mean absolute error ($E_{mae}$). $E_{mae}$ is used as the fit equation to evaluate the fit of numerical results and is defined as (Ren *et al*. 2022).

$$E_{mae} = \left|\frac{R_{L_i} - R_{FEM_i}}{R_{L_i}}\right| x100, (i = 1,2,3,\ldots,n) \quad (1)$$

where $R_{Li}$ and $R_{FEMi}$ are the literature and FEM results, respectively. $n$ denotes the total number of results.

Different values were used for each bacteria. The constant values used are as follows;

*E. coli:* height (200 nm), width (50 nm), peak radius (25 nm), spacing (500 nm),

*P. aeruginosa:* height (250 nm), width (50 nm), peak radius (25 nm), spacing (250 nm),

*S. aureus:* height (100 nm), width (50 nm), peak radius (25 nm), spacing (130 nm).

Fig. 5 shows the change in maximum stress, strain, and deformation versus nanopattern width, considering the following parameters: (Peak sharpness=STS, spacing=300 nm, material=Zr). It is seen that stress, strain, and deformation increase with the decrease of the width. The same trend is valid for the three bacterial species. When we compare bacteria, it is seen that the highest values are in *E. coli*, then in *P. aeruginosa*, and the smallest values in *S. aureus*. Similar to the report of Velic *et al*. (2021), reducing the nanopattern width in this study seems to be a successful strategy to increase the bactericidal effect of the modeled nanopatterned surfaces.

Fig. 6 demonstrates the change in the maximum stress,

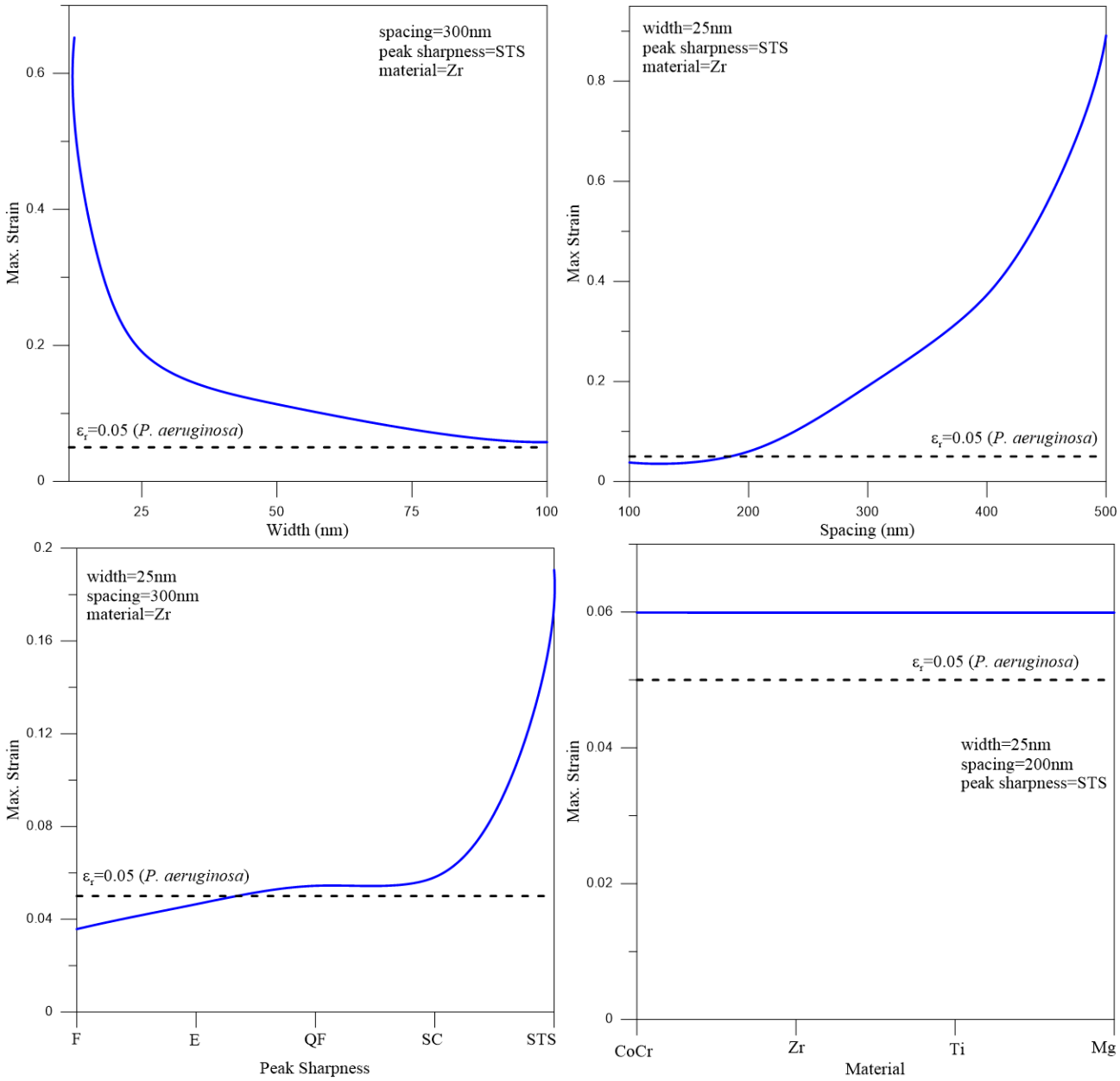


Fig. 10 Parametric analysis (width, spacing, peak sharpness, and material) of *P. aeruginosa* for mortality, taking into account strain

strain, and deformation against the spacing of nanopattern considering the following non-dimensional parameters: (Width=25 nm, peak sharpness=STS, material=Zr). The tips will behave like a flat surface if the spacing between nanopatterns is small. High density can lead to a "nail bed" effect where the bactericidal effect of individual columns is reduced (Linklater *et al*. 2021). Conversely, some experimental studies have shown that decreasing spacing increases killing efficacy (Dickson *et al*. 2015). This study shows that stress, strain, and deformation increase with increasing distance for Gram-negative bacteria (*E. coli* and *P. aeruginosa*). On the contrary, it is seen that stress, strain, and deformation decrease with increasing spacing for gram-positive bacteria (*S. aureus)*. This can be explained by the fact that if the spacing in the nanopattern is larger than the size of the cell, bacteria can fall in and avoid the bactericidal effect by reducing the contact surface.

Fig. 7 presents the maximum stress, strain, and deformation change against the peak sharpness of the nanopattern considering the following parameters: (Width =25 nm, spacing=300 nm, material=Zr). It was found that, as the peak sharpness increased, stress, strain, and deformation increased for all bacteria (*E. coli*, *P. aeruginosa*, *S. aureus*). The highest increase was observed in *E. coli*, followed by *P. aeruginosa* and *S. aureus*.

Fig. 8 shows the maximum stress, strain, and deformation change against the material properties (CoCr, Zr, Ti, Mg) considering the following parameters: (Width =25 nm, spacing=200 nm, peak sharpness=STS). It was determined that using different materials for the nano-

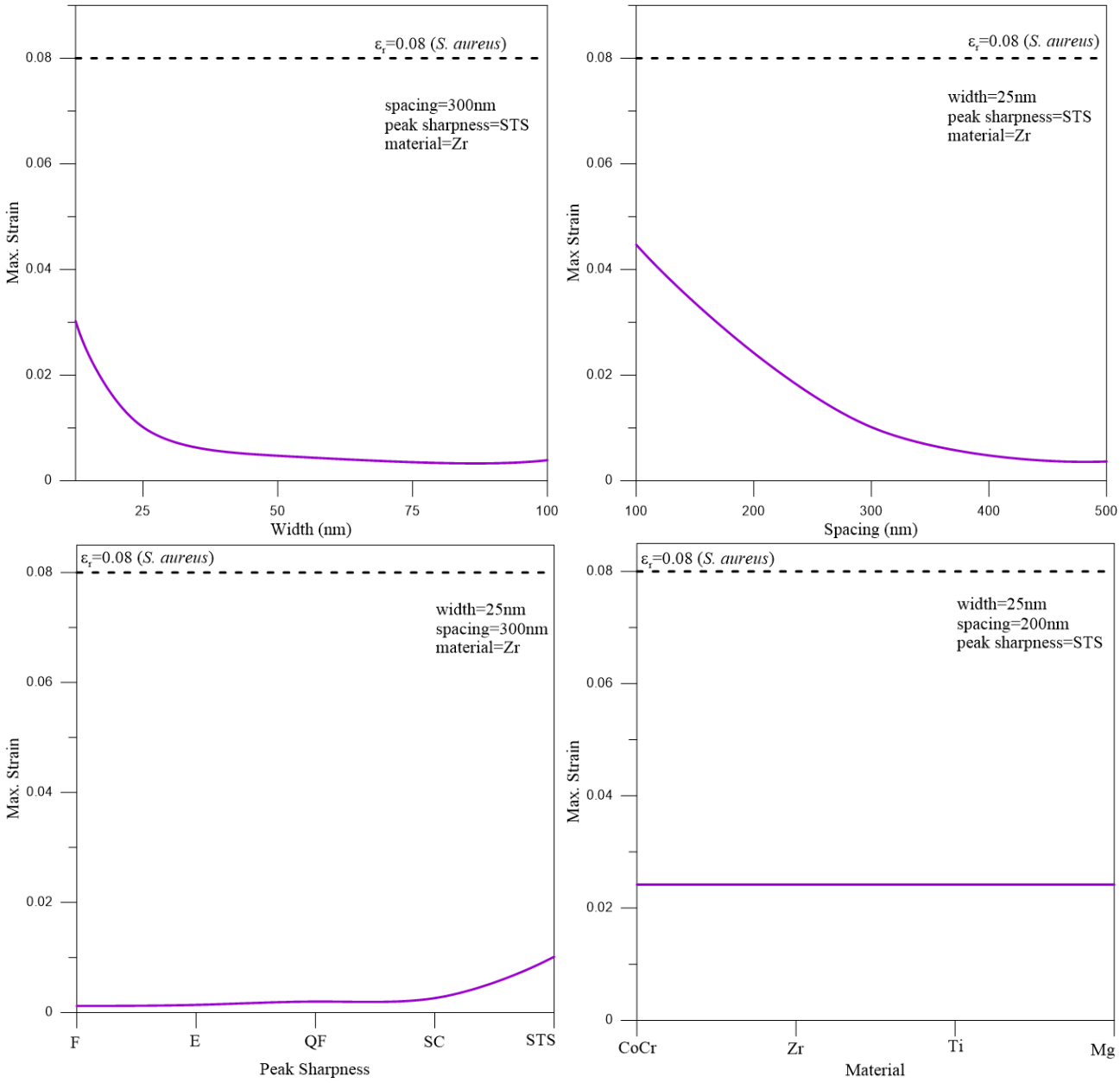


Fig. 11 Parametric analysis (width, spacing, peak sharpness, and material) of *S. aureus* for mortality, taking into account strain

pattern did not significantly change the stress, strain, and deformation.

It was considered that a bacteria could be inactivated if the equivalent von -Mises strain (εeq) determined within the bacterial wall exceeded the rupture threshold stress (εr). AFM force measurement analyses can determine the threshold values of bacteria. In literature, threshold values were measured as εr = 0.12 for *E. coli* (Turner *et al*. 2013), εr = 0.05 for *P. aeruginosa* (Gumbart *et al*. 2014), and εr = 0.08 for *S. aureus* (Bailey *et al*. 2014).

In Fig. 9, three graphs showed increased mortality in *E. coli* cells. 1) while the spacing=300 nm, peak sharpness =STS, material=Zr values are constant, when the diameter is below ~50 nm; 2) diameter=25 nm, peak sharpness=STS, material=Zr, when the spacing increased above ~200 nm; 3) diameter=25 nm, spacing=300 nm, material=Zr values were constant, while the peak sharpness was STS. In addition, while diameter=25 nm, spacing=200 nm, and peak sharpness =STS values were constant, no mortality was observed even with the material change.

In Fig. 10, three graphs showed increased mortality in *P. aeruginosa* cells. 1) while the spacing=300 nm, peak sharpness=STS, material=Zr values are constant, when the diameter is below ~100 nm; 2) diameter=25 nm, peak sharpness=STS, material=Zr values, when the spacing exceeds ~200 nm; 3) diameter=25 nm, spacing =300 nm, material=Zr values were constant, while the peak sharpness was E-STS. In addition, diameter=25 nm, spacing=200 nm, and peak sharpness =STS values remained constant, although no mortality was observed in *P. aeruginosa* cells despite the material change.

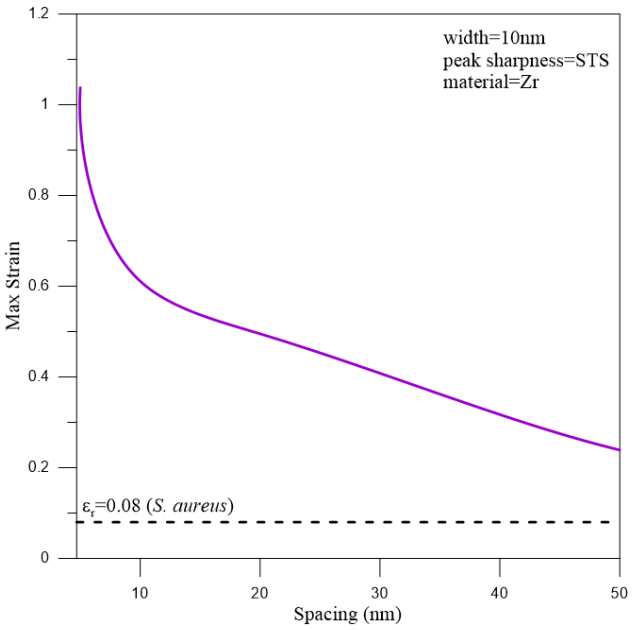


Fig. 12 *S. aureus* for mortality, taking into account strain

Fig. 11 shows that *S. aureus* cells do not die under any condition where the model bacteria used in the study (*E. coli* and *P. aeruginosa*) show mortality. Additional analyses were performed for *S. aureus* bacteria. Values at which mortality could be observed were calculated.

Fig. 12 shows the extra analyses performed to monitor mortality in *S. aureus* cells. Here, while diameter=10 nm, peak sharpness=STS, and material=Zr values are constant, mortality is observed in *S. aureus* cells at values below the spacing below ~50 nm.

## 4. Conclusions

In this study, the mechanical effects of the geometric parameters (peak sharpness, height, width, and spacing) and material properties (chrome-cobalt, zirconium, titanium, and magnesium) of nanopatterned surfaces on bacterial cells (*E. coli*, *P. aeruginosa*, and *S. aureus*) were investigated. The mechano-bactericidal effect was calculated by FEM. Elastic and creep deformation models of bacterial cells adhered to the nano surface were created, and cell deformation, stress, strain, and mortality were calculated. The results showed that sharpening the peak sharpness and decreasing the width of the nanopatterns increased the maximum deformation, stress, and strain in the walls of the three bacterial cells. The increase in spacing between nanopatterns increased the maximum deformation, stress, and strain in *E. coli* and *P. aeruginosa* cell walls; it decreased the same values in *S. aureus*. However, the increase in spacing between nanopatterns decreased the maximum deformation, maximum stress, and maximum strain in the *S. aureus* cell wall. While the decrease in width with the increase in sharpness and spacing increases the mortality of *E. coli* and *P. aeruginosa* cells, the same values did not cause mortality in *S. aureus* cells. In this study, mortality values of *S. aureus* cells were calculated by performing additional analyses. Using different materials for the nanopattern did not cause a significant change in stress, strain, and deformation.

Nano-patterned surfaces show the potential to be used as an antibacterial material in implants in terms of not showing toxic effects and bacterial resistance. In this study, computer modeling of both the geometric structures and material properties of nano-patterned surfaces will accelerate and promote the design of more efficient mechano-bactericidal implant surfaces in the future.

## Acknowledgments

The research of the corresponding author is supported by a grant from Ferdowsi University of Mashhad (N2. 59254)

## References

Alameda, M.T., Osorio, M.R., Pedraz, P. and Rodríguez, I. (2022), "Mechano-dynamic analysis of the bactericidal activity of bioinspired moth-eye nanopatterned surfaces", *Adv. Mater. Interf.*, **9**, 2270127. https://doi.org/10.1002/admi.202270127.

Alaneme, K.K., Kareem, S.A., Olajide, J.L., Sadiku, R.E. and Bodunrin, M.O. (2022), "Computational biomechanical and biodegradation integrity assessment of Mg-based biomedical devices for cardiovascular and orthopedic applications: A review", *Int. J. Lightweight Mater. Manuf.*, **5**(2), 251-266. https://doi.org/10.1016/j.ijlmm.2022.02.003.

Altabey, W.A., Noori, M., Alarjani, A. and Zhao, Y. (2020), "Nano-delamination monitoring of BFRP nano-pipes of electrical potential change with ANNs", *Adv. Nano Res.*, **9**(1), 1-13. https://doi.org/10.12989/ANR.2020.9.1.001.

ANSYS (2013), *Mechanical APDL, ANSYS Contact Technology Guide*, Ansys, Inc., Canonsburg, Pennsylvania, U.S.A.

Bailey, R.G., Turner, R.D., Mullin, N., Clarke, N., Foster, S.J. and Hobbs, J.K. (2014), "The interplay between cell wall mechanical properties and the cell cycle in *Staphylococcus aureus*", *Biophys. J.*, **107**(11), 2538-2545. https://doi.org/10.1016/j.bpj.2014.10.036.

Bouafia, H., Chikh, A., Bousahla, A.A., Bourada, F., Heireche, H., Tounsi, A., Benrahou, K.H., Tounsi, A., Al-Zahrani, M.M. and Hussain, M. (2021), "Natural frequencies of FGM nanoplates embedded in an elastic medium", *Adv. Nano Res.*, **11**(3), 239-249. https://doi.org/ 10.12989/anr.2021.11.3.239.

Callister, W.D. and Rethwisch, D.D. (2013), *Materials Science and Engineering*, Nobel Akademik Yayıncılık, 8, Baskı.

Cayley, S., Lewis, B.A., Guttman, H.J. and Record Jr, M.T. (1991), "Characterization of the cytoplasm of *Escherichia coli* K-12 as a function of external osmolarity. Implications for protein-DNA interactions in vivo", *J. Mol. Biol.*, **222**(2), 281-300. https://doi.org/10.1016/0022-2836(91)90212-o.

Cerioli, M., Batailler, C., Conrad, A., Roux, S., Perpoint, T., Becker, A., Triffault-Fillit, C., Lustig, S., Fessy, M.H., Laurent, F., Valour, F., Chidiac, C. and Ferry, T. (2020), "*Pseudomonas aeruginosa* implant-associated bone and joint infections: experience in a regional reference center in France", *Front. Med.*, **7**. https://doi.org/10.3389/fmed.2020.513242.

Chouirfa, H., Bouloussa, H., Migonney, V. and Falentin-Daudré, C. (2019), "Review of titanium surface modification techniques and coatings for antibacterial applications", *Acta Biomater.*, **83**, 37-54. https://doi.org/10.1016/j.actbio.2018.10.036.

Colling, E.W., (1984), "The Physical Metallurgy of Titanium Alloys, Metals Park (OH)", *Am. Soc. Metals*, 65-72.

Crémet, L., Corvec, S., Bémer, P., Bret, L., Lebrun, C., Lesimple,

B., Miegeville, A.F., Reynaud, A., Lepelletier, D. and Caroff, N. (2012), "Orthopaedic-implant infections by Escherichia coli: molecular and phenotypic analysis of the causative strains", *J. Infect.*, **64**(2), 169-175. https://10.1016/j.jinf.2011.11.010.

Cui, Q., Liu, T., Li, X., Zhao, L., Wu, Q., Wang, X., Song, K. and Ge, D. (2021), "Validation of the mechano-bactericidal mechanism of nanostructured surfaces with finite element simulation", *Colloids Surf. B*, **206**, 111929. https://doi.org/10.1016/j.colsurfb.2021.111929.

De Breij, A., Riool, M., Kwakman, P.H.S., De Boer, L., Cordfunke, R.A., Drijfhout, J.W., Cohen, O., Emanuel, N., Zaat, S.A., Nibbering, P.H. and Moriarty, T.F. (2016), "Prevention of Staphylococcus aureus biomaterial-associated infections using a polymer-lipid coating containing the antimicrobial peptide OP-145", *J. Control Release*, **222**, 1-8. https://doi.org/10.1016/j.jconrel.2015.12.003.

Dickson, M.N., Liang, E.I., Rodriguez, L.A., Vollereaux, N. and Yee, A.F. (2015), "Nanopatterne polymer surfaces with bactericidal properties", *Biointerphases*, **10**(2), 021010. https://doi.org/10.1116/1.4922157.

Donlan, R.M. (2002), "Biofilms: microbial life on surfaces", *Emerg. Infect. Dis.*, **8**(9), 881-890. https://doi.org/10.3201/eid0809.020063.

Eltaher, M.A., Almalki, T.A., Ahmed, K.I.E. and Almitani, K.H. (2019), "Characterization and behaviors of single walled carbon nanotube by equivalent-continuum mechanics approach", *Adv. Nano Res.*, **7**(1), 39. https://doi.org/10.12989/anr.2019.7.1.039.

Ghanbari, A., Dehghany, J., Schwebs, T., Müsken, M., Häussler, S. and Meyer-Hermann, M. (2016), "Inoculation density and nutrient level determine the formation of mushroom-shaped structures in *Pseudomonas aeruginosa* biofilms", *Sci. Rep.*, **6**, 32097. https://doi.org/10.1038/srep32097.

Gumbart, J.C., Beeby, M., Jensen, G.J. and Roux, B. (2014), "*Escherichia coli* peptidoglycan structure and mechanics as predicted by atomic-scale simulations", *PLoS Comput Biol.*, **10**(2), e1003475. https://doi.org/10.1371/journal.pcbi.1003475.

Güvercin, Y., Abdioğlu, A.A., Dizdar, A., Uzun Yaylacı, E. and Yaylacı, M. (2022a), "Suture button fixation method used in the treatment of syndesmosis injury: A biomechanical analysis of the effect of the placement of the button on the distal tibiofibular joint in the mid-stance phase with finite elements method", *Injury*, **53**(7), 2437-2445 https://doi.org/10.1016/j.injury.2022.05.037.

Güvercin, Y., Yaylacı, M., Dizdar, A., Kanat, A., Uzun Yaylacı, E., Ay, S., Abdioğlu, A.A. and Şen, A. (2022b), "Biomechanical analysis of odontoid and transverse atlantal ligament in humans with ponticulus posticus variation under different loading conditions: finite element study", *Injury*, **53**, 3879-3886. https://doi.org/10.1016/j.injury.2022.10.003.

Hansen, E.N., Zmistowski, B. and Parvizi, J. (2012), "Periprosthetic joint infection: What is on the horizon?", *Int. J. Artif. Organs*, **35**(10), 935-950. https://doi.org/10.5301/ijao.5000145.

Ivanova, E.P., Linklater, D.P., Werner, M., Baulin, V.A., Xu, X., Vrancken, N., Rubanov, S., Hanssen, E., Wandiyanto, J., Truong, V.K., Elbourne, A., Maclaughlin, S., Juodkazis, S. and Crawford, R.J. (2020), "The multi-faceted mechano-bactericidal mechanism of nanostructured surfaces", *Proc. Natl. Acad. Sci. U.S.A.*, **117**(23), 12598-12605. https://doi.org/10.1073/pnas.1916680117.

Kuiper, J.W., Willink, R.T., Moojen, D.J., van den Bekerom, M.P. and Colen, S. (2014), "Treatment of acute periprosthetic infections with prosthesis retention: Review of current concepts", *World J. Orthop.*, **5**(5), 667-676. https://doi.org/10.5312/wjo.v5.i5.667.

Kuma, Y., Gupta, A. and Tounsi, A. (2021), "Size-dependent vibration response of porous graded nanostructure with FEM and nonlocal continuum model", *Adv. Nano Res.*, **11**(1), 1-17. https://doi.org/10.12989/ANR.2021.11.1.001.

Li, X. (2016), "Bactericidal mechanism of nanopatterned surfaces", *Phys. Chem. Chem. Phys.*, **18**(2), 1311-1316. https://doi.org/10.1039/C5CP05646B.

Li, X., Wu, B., Chen, H., Nan, K., Jin, Y., Sun, L. and Wang, B. (2018), "Recent developments in smart antibacterial surfaces to inhibit biofilm formation and bacterial infections", *J. Mater. Chem. B*, **6**(26), 4274-4292. https://doi.org/10.1039/C8TB01245H.

Linklater, D.P., Baulin, V.A., Juodkazis, S., Crawford, R.J., Stoodley, P. and Ivanova, E.P. (2021), "Mechano-bactericidal actions of nanostructured surfaces", *Nat. Rev. Microbiol.*, **19**(1), 8-22. https://doi.org/10.1038/s41579-020-0414-z.

Maleki, E., Mirzaali, M.J., Guagliano, M. and Bagherifard, S. (2021), "Analyzing the mechano-bactericidal effect of nano-patterned surfaces on different bacteria species", *Surf. Coat. Technol.*, **408**. https://doi.org/10.1016/j.surfcoat.2020.126782.

Mehar, K. and Panda, S.K. (2019), "Multiscale modeling approach for thermal buckling analysis of nanocomposite curved structure", *Adv. Nano Res.*, **7**(3), 181-190. https://doi.org/10.12989/ANR.2019.7.3.181.

Mirzaali, M.J., van Dongen, I.C.P., Tumer, N., Weinans, H., Yavari, S.A. and Zadpoor, A.A. (2018), "In-silico quest for bactericidal but non-cytotoxic nanopatterns", *Nanotechnology*, **29**, 43LT02. https://doi.org/10.1088/1361-6528/aad9bf.

Pandey, H.K., Hirwani, C.K., Sharma, N., Katariya, P.V., Dewangan, H.C. and Panda, S.K. (2019), "Effect of nano glass cenosphere filler on hybrid composite eigenfrequency responses - An FEM approach and experimental verification", *Adv. Nano Res.*,**7**(6), 419-429. https://doi.org/10.12989/ANR.2019.7.6.419.

Pogodin, S., Hasan, J., Baulin, V.A., Webb, H.K., Truong, V.K., Phong Nguyen, T.H., Boshkovikj, V., Fluke, C.J., Watson, G.S., Watson, J.A., Crawford, R.J. and Ivanova, E.P. (2013), "Biophysical model of bacterial cell interactions with nano-patterned cicada wing surfaces", *Biophys. J.*, **104**(4), 835–840. https://doi.org/10.1016/j.bpj.2012.12.046.

Ren, W., Wu, X. and Cai, R. (2022), "A hybrid artificial intelligence and IOT for investigation dynamic modeling of nano-system", *Adv. Nano Res.*, **13**(2), 165-174. https://doi.org/10.12989/anr.2022.13.2.165.

Roy, A. and Chatterjee, K., (2021), "Theoretical and computational investigations into mechanobactericidal activity of nanostructures at the bacteria-biomaterial interface: A critical review", *Nanoscale*, **13**, 647. https://doi.org/10.1039/D0NR07976F.

Turner, R.D., Hurd, A.F., Cadby, A., Hobbs, J.K. and Foster, S.J. (2013), "Cell wall elongation mode in Gram-negative bacteria is determined by peptidoglycan architecture", *Nat. Commun.*, **4,** 1496. https://doi.org/10.1038/ncomms2503.

Uzun Yaylacı, E., Yaylacı, M., Özdemir, M.E., Terzi, M. and Öztürk, Ş. (2023), "Analyzing the mechano-bactericidal effect of nano-patterned surfaces by finite element method and verification with artificial neural networks" *Adv. Nano Res.*, **15**(2), 165-174. https://doi.org/10.12989/anr.2023.15.2.165.

Vadillo-Rodriguez, V., Schooling, S.R. and Dutcher, J.R. (2009), "In situ characterization of differences in the viscoelastic response of individual gram-negative and gram-positive bacterial cells", *J. Bacteriol.*, **191**(17), 5518-5525. https://doi.org/10.1128/JB.00528-09.

Velic, A., Hasan, J., Li, Z. and Yarlagadda, P. (2021), "Mechanics of bacterial interaction and death on nanopatterned surfaces", *Biophys. J.*, **120**, 217-231. https://doi.org/10.1016/j.bpj.2020.12.003.

Westberg, M., Frihagen, F., Brun, O.C., Figved, W., Grøgaard, B., Valland, H., Wangen, H. and Snorrason, F. (2015), "Effectiveness of gentamicin-containing collagen sponges for prevention

of surgical site infection after hip arthroplasty: A multicenter randomized trial", *Clin. Infect. Dis.*, **60**(12), 1752-1759. https://doi.org/10.1093/cid/civ162.

Whatmore, A.M. and Reed, R.H. (1990), "Determination of turgor pressure in Bacillus subtilis: a possible role for K+ in turgor regulation", *J. Gen. Microbiol.*, **136**(12), 2521-2526. https://doi.org/10.1099/00221287-136-12-2521.

Xia, L., Wang, R., Chen, G., Asemi, K. and Tounsi, A. (2023), "The finite element method for dynamics of FG porous truncated conical panels reinforced with graphene platelets based on the 3-D elasticity", *Adv. Nano Res.*, **14**(4), 375-389. https://doi.org/10.12989/.2023.14.4.375.

Yao, X., Jericho, M., Pink, D. and Beveridge, T. (1999), "Thickness and elasticity of gram-negative murein sacculi measured by atomic force microscopy", *J. Bacteriol.*, **181**(22), 6865-6875. https://doi.org/10.1128/JB.181.22.6865-6875.1999.

Yao, X., Walter, J., Burke, S., Stewart, S., Jericho, M.H., Pink, D., Hunter, R. and Beveridge, T.J. (2002), "Atomic force microscopy and theoretical considerations of surface properties and turgor pressures of bacteria", *Colloids Surf. B*, **23**(2-3), 213-230. https://doi.org/10.1016/S0927-7765(01)00249-1.

Yaylacı, M. (2022), "Simulate of edge and an internal crack problem and estimation of stress intensity factor through finite element method", *Adv. Nano Res.*, **12**(4), 405-414. https://doi.org/10.12989/anr.2022.12.4.405.

Yaylacı, M., Abanoz, M., Uzun Yaylacı, E., Ölmez, H., Sekban, M.D. and Birinci, A. (2022a), "The contact problem of the functionally graded layer resting on rigid foundation pressed via rigid punch", *Steel Compos. Struct.*, **43**(5), 661-672. https://doi.org/10.12989/scs.2022.43.5.661.

Yaylacı, M., Şengül Şabano, B., Özdemir, M.E. and Birinci, A. (2022b), "Solving the contact problem of functionally graded layers resting on a homogeneous half-plane and pressed with a uniformly distributed load by analytical and numerical methods", *Struct. Eng. Mech.*, **82**(3), 401-416. https://doi.org/10.12989/sem.2022.82.3.401.

Yaylacı, M., Uzun Yaylacı, E., Özdemir, M.E., Ay, S. and Öztürk, Ş. (2022c), "Implementation of finite element and artificial neural network methods to analyze the contact problem of a functionally graded layer containing crack", *Steel Compos. Struct.*, **45**(4), 501-511. https://doi.org/10.12989/scs.2022.45.4.501.

Yaylacı, M., Yaylı, M., Uzun Yaylacı, E., Ölmez, H. and Birinci, A. (2021), "Analyzing the contact problem of a functionally graded layer resting on an elastic half plane with theory of elasticity, finite element method and multilayer perceptron", *Struct. Eng. Mech.*, **78**(5), 585-597. https://doi.org/10.12989/sem.2021.78.5.585.

Zagane, M.S., Moulgada, A., Yaylacı, M., Abderahmen, S., Özdemir, M.E., Uzun Yaylacı, E., (2023), "Numerical simulation of the total hip prosthesis under static and dynamic loading (for three activities)", *Struct. Eng. Mech.*, **86**(5). https://doi.org/10.12989/sem.2023.86.5.000.

Zhao, J., Tang, J., Zhou, W., Jiang, T., Wu, H., Liao, X. and Guo, M. (2022), "Surface integrity of gear shot peening considering complex geometric conditions: A sequential coupled DEM-FEM method", *Surf. Coat. Technol.*, **449**. https://doi.org/10.1016/j.surfcoat.2022.128943.

Zhou, C., Koshani, R., O'Brien, B., Ronholm, J., Cao, X. and Wang, Y. (2021), "Bio-inspired mechano-bactericidal nano-structures: A promising strategy for eliminating surface food-borne bacteria", *Curr. Opin. Food Sci.*, **39**, 110-119. https://doi.org/10.1016/j.cofs.2020.12.021.